Mammalian Aging (Prentice-Hall, Englewood Cliffs, N.J., 1971); S. Goldstein, *N. Engl. J. Med.* **285**, 1120 (1971); and the comprehensive review by Cristofalo (*9*)].
7. L. Hayflick and P. S. Moorhead, *Exp. Cell Res.* **25**, 585 (1961).
8. L. Hayflick, *ibid.* **37**, 614 (1965).
9. V. J. Cristofalo, *Advan. Gerontol. Res.* **4**, 45 (1972).
10. G. M. Martin, C. A. Sprague, C. J. Epstein, *Lab. Invest.* **23**, 86 (1970).
11. G. S. Merz and J. D. Ross, *J. Cell. Physiol.* **74**, 219 (1969).
12. A. Macieira-Coelho, J. Pontén, L. Philipson, *Exp. Cell Res.* **43**, 20 (1966).
13. ———, *ibid.* **42**, 673 (1966); A. Macieira-Coelho and J. Pontén, *J. Cell Biol.* **43**, 374 (1969); A. Macieira-Coelho, in *Aging in Cell and Tissue Culture*, E. Holečková and V. J. Cristofalo, Eds. (Plenum, New York, 1970), pp. 121–132.
14. L. N. Zhinkin and L. F. Andreeva, *J. Embryol. Exp. Morphol.* **11**, 353 (1963).
15. S. P. Modak, G. Morris, T. Yamada, *Develop. Biol.* **17**, 544 (1968).
16. L. N. Zhinkin, quoted by Epifanova and Terskikh (*1a*).
17. J. Post and J. Hoffman, *Exp. Cell Res.* **40**, 333 (1965).
18. ———, *ibid.* **36**, 111 (1964); *Progr. Liver Dis.* **2**, 155 (1965).
19. E. A. Tonna, *J. Biophys. Cytol.* **9**, 813 (1961).
20. H. E. Enesco, *J. Gerontol.* **22**, 445 (1967).
21. L. von Sallmann and P. Grimes, *Invest. Ophthalmol.* **5**, 560 (1966).
22. C. Desaive, *C. R. Hebd. Seances Acad. Sci.* **260**, 315 (1965).
23. H. J. Whitely and D. L. Horton, *J. Gerontol.* **18**, 335 (1963).
24. J. D. Thrasher and R. C. Greulich, *J. Exp. Zool.* **159**, 39 (1965); *ibid.*, p. 385.
25. J. Post and J. Hoffman, *Radiat. Res.* **45**, 335 (1971).
26. T. Pederson and S. Gelfant, *Exp. Cell Res.* **59**, 32 (1970).
27. H. A. Johnson and J. M. Vera Roman, *Amer. J. Pathol.* **49**, 1 (1966).
28. This statement is based upon many experiments with mouse epidermis, kidney, and duodenum. It also seems to apply to a variety of other tissues (*4, 26*).
29. S. Lesher and G. A. Sacher, *Exp. Gerontol.* **3**, 211 (1968).
30. A. Balázs and G. Rappay, *ibid.*, p. 1.
31. J. F. Albright and T. Makinodan, *J. Cell. Physiol.* **67** (Suppl. 1), 185 (1966); E. H. Perkins and T. Makinodan, *Proceedings, First Rocky Mountain Symposium on Aging* (in press). G. B. Price and T. Makinodan [*J. Immunol.* **108**, 403 (1972)] demonstrate that decrease in the number of antibody-producing cells in old mice is due in part to decrease in the proliferation of precursor immunocompetent cells.
32. B. Messier and C. P. Leblond, *Amer. J. Anat.* **106**, 247 (1960); J. L. Edwards and R. E. Klein, *Amer. J. Pathol.* **38**, 437 (1961).
33. J. Post and J. Hoffman, *N. Engl. J. Med.* **279**, 248 (1968).
34. L. N. Castor, *J. Cell. Physiol.* **72**, 161 (1968).
35. Hayflick's ideas (*8*) are also being questioned for other reasons. For example, L. M. Franks [*Exp. Gerontol.* **5**, 281 (1970)] and L. Lima and A. Macieira-Coelho [*Exp. Cell Res.* **70**, 279 (1972)] point out that rodent and chick fibroblasts differ in some respects from human fibroblasts in their "aging" in vitro, and J. S. McHale, M. L. Mouton, and J. T. McHale [*Exp. Gerontol.* **6**, 89 (1971)] indicate that the limited culture life-span of human diploid cells may be a function of metabolic time instead of cell division potential. Also, Cameron (*36*) emphasizes that Hayflick's concept of a finite number of cell population doublings in vitro (about 50) may not apply to normal diploid cells in vivo.
36. I. L. Cameron, *J. Gerontol.* **27**, 157 (1972).
37. V. J. Cristofalo, in *Aging in Cell and Tissue Culture*, E. Holečková and V. J. Cristofalo, Eds. (Plenum, New York, 1970), pp. 83–119; A. Macieira-Coelho, *Experientia* **22**, 390 (1966); C. Arpels, V. I. Babcock, C. M. Southam, *Proc. Soc. Exp. Biol. Med.* **115**, 102 (1964).
38. J. J. DeCosse and S. Gelfant, *Proc. Amer. Ass. Cancer Res.* **7**, 17 (1966).
39. Regeneration produced by partial hepatectomy is described by N. L. R. Bucher [*N. Engl. J. Med.* **227**, 686 (1967); *ibid.*, p. 738; also (*40*)]; for regeneration after partial nephrectomy see C. E. McCreight and N. M. Sulkin [*Amer. J. Anat.* **110**, 199 (1962)], and Johnson and Vera Roman (*27*). Post *et al.* (*41*) describe regeneration produced by chemical removal of tissue by necrosis and the effects of carbon tetrachloride on the liver; F. E. Cuppage, N. Cunningham, A. Tate [*Lab. Invest.* **21**, 449 (1969)] describe kidney regeneration produced with mercuric chloride.
40. N. L. R. Bucher, *Int. Rev. Cytol.* **15**, 245 (1963).
41. J. Post, A. Klein, J. Hoffman, *Arch. Pathol.* **70**, 314 (1960).
42. For release of liver cells see (*3, 40, 41*); for release of G_1 or G_2 blocked kidney cells see T. Pederson and S. Gelfant [*J. Cell Biol.* **35**, 101A (1967)]; also (*43*).
43. C. E. McCreight and N. M. Sulkin, *J. Gerontol.* **14**, 440 (1959); T. L. Phillips and G. F. Leong, *Cancer Res.* **27**, 286 (1967).
44. N. L. R. Bucher and A. D. Glinos, *Cancer Res.* **10**, 324 (1950); N. L. R. Bucher, M. N. Swaffield, J. F. DiTroia, *ibid.* **24**, 509 (1964).
45. D. J. Ingle and B. L. Baker, *Proc. Soc. Exp. Biol. Med.* **95**, 813 (1957).
46. H. V. Samis, Jr., J. A. Falzone, V. J. Wulff, *Gerontologia* **12**, 79 (1966).
47. T. Pederson and S. Gelfant, *J. Cell Biol.* **31**, 84A (1966); also unpublished results.
48. Supported by NIH grants AM 16060, AM 05586, and AM 12062.

Fourier Transform Spectroscopy

New methods dramatically improve the sensitivity of infrared and nuclear magnetic resonance spectroscopy.

Edwin D. Becker and T. C. Farrar

In the last year or so a wealth of new information about the structure of molecular systems has become available as a result of the recent dramatic 10- to 100-fold increase in the sensitivity of infrared (IR) and nuclear magnetic resonance (NMR) spectrometers. The development that has made this possible is generally called Fourier transform (FT) spectroscopy; it is also sometimes termed interferometry or time-domain spectroscopy. Although interferometric methods in optical spectroscopy have been well known and understood since the early work of Michelson (*1*), the widespread application of these techniques has become possible only recently with the development of the necessary instrumentation and of fast, inexpensive computers.

In this article we describe the FT method, provide some insight into the elementary theory and instrumentation involved, and give some examples of the ways in which FT spectroscopy is beginning to make an impact on chemical and biochemical research. We shall first treat briefly FT-IR spectroscopy, since the concepts involved in optical methods are somewhat more familiar and easier to grasp. However, the major part of this article will be devoted to NMR (*2*).

The basic power of FT spectroscopy arises, quite simply, from the fact that it is very much faster than frequency-domain or conventional methods. In conventional ^{13}C NMR spectroscopy, for example, it would require about 5000 seconds to obtain a complete spectrum with a resolution of 1 hertz. The same basic spectral information can be obtained in 1 second with the use of FT methods. In addition, the general quality of the spectrum (especially line shape) obtained in this very much shorter time is appreciably better. This great saving in time may be exploited in improving the signal-to-noise ratio (*S/N*) by the coherent addition of signals, since random noise tends to cancel. Such coherent addition, or "time averaging," can indeed be carried out with conventional spectroscopy as well, but often only with an expenditure of time that makes the experiment prohibitive. In the ^{13}C

Dr. Becker is chief of the Laboratory of Chemical Physics, National Institute of Arthritis, Metabolism, and Digestive Diseases, National Institutes of Health, Bethesda, Maryland 20014. Dr. Farrar is director of research and development, JEOL, Inc., Cranford, New Jersey 07016.

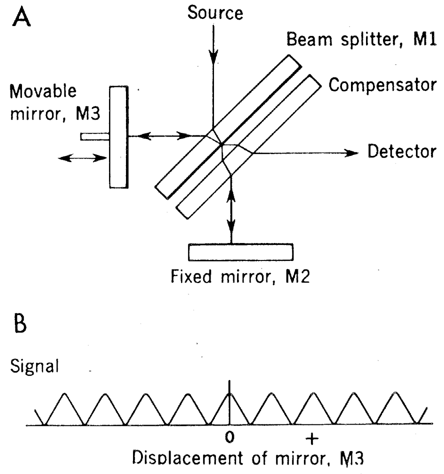

Fig. 1. (A) Schematic diagram of a Michelson interferometer. (B) Signal obtained as a function of mirror displacement for a monochromatic wave.

NMR example cited it is often necessary to sum the data from a thousand repetitive scans; this procedure requires about 15 minutes in the FT mode, but 60 days by conventional spectroscopy to achieve comparable S/N and resolution in the final spectra (*3*).

Infrared Interferometry

The equipment used in FT-IR spectroscopy consists of a Michelson interferometer, a simple arrangement of mirrors of the type depicted in Fig. 1A. The "beam splitter," M1, behaves like a half-silvered mirror, so that half the energy from the incident beam is transmitted to M2 while half is reflected to M3. Consider a monochromatic beam incident on M1. If the path length from M1 to M2 is exactly equal to the path length from M1 to M3, then the reflected beams add coherently in phase at M1. If, however, there is a path-length difference of $\lambda/4$, where λ is the wavelength of the radiation, then one reflected beam traverses an extra distance $\lambda/2$ before arriving at M1 and interferes destructively with the second reflected beam. Thus, if M2 remains fixed while M3 is moved at a constant rate, the signal at the detector is a cosine wave, as shown in Fig. 1B. If the source consists of radiation with more than a single wavelength, the distances of mirror displacement at which constructive and destructive interference occur vary with wavelength, as indicated in Fig. 2, and the resulting signal from the interference of these separate waves is termed an interferogram. If the source gives rise to many closely spaced frequencies (a continuous, broad-band source), interference effects cause the signal to decay rapidly as the mirror moves away from the zero fringe, where all waves are in phase. When a sample is placed between the interferometer and the detector, it absorbs some of the frequencies present. The result is a modified interference pattern.

It is clear that the exact shape of the interferogram depends on the frequencies present in the spectrum, and a little further thought shows that the amplitude, or intensity, of each component frequency is also important. Thus, the interferogram contains the basic information on frequencies and intensities characteristic of the spectrum but in a form that is not directly interpretable. Fourier transform methods make it possible to convert the information to a more familiar form.

The Fourier transform, $F(\omega)$, of a function, $f(t)$, is given by

$$F(\omega) = \int_{-\infty}^{\infty} f(t)e^{-i\omega t}dt$$

where the imaginary exponential is

$$e^{i\omega t} = \cos \omega t + i \sin \omega t$$

The two functions, $f(t)$ and $F(\omega)$, are said to constitute a Fourier transform pair, the former in the time domain and the latter in the frequency domain. They both contain the same physical information; they merely express it in different ways. If

$$f(t) = A \cos \omega_0 t$$

then $F(\omega)$ is a single line at ω_0 with its amplitude proportional to A. Likewise the Fourier transform of the interferogram shown in Fig. 2 is a set of three lines at the frequencies of the component waves.

In practice the Fourier transformation is normally carried out in a digital computer by means of a summation over a finite number of points, N:

$$F(\omega_j) = \sum_{k=1}^{N} f(t_k)\, e^{-i\omega_j t_k}\ ; j = 0, 1, \ldots N$$

In order that this discrete Fourier transform generate the true $F(\omega)$, it is important not only that the total number of data points, N, be large enough but also that the data be obtained at a fast enough rate. The reason for this requirement on the rate of data acquisition is easily seen. If we wish to represent in digital form a cosine wave of frequency ν_j hertz ($\omega_j = 2\pi\nu_j$ radians per second), the sampling theorem (*4*) tells us that we must take two data points per cycle to specify the amplitude and frequency of the wave. A larger number of points per cycle provides no additional information but does not in any way detract from the information content. A sampling rate of fewer than two points per cycle, however, introduces ambiguity and results in a distortion of the spectrum. Thus, if it is known that $\nu_{\max}$ is the highest frequency present, the minimum

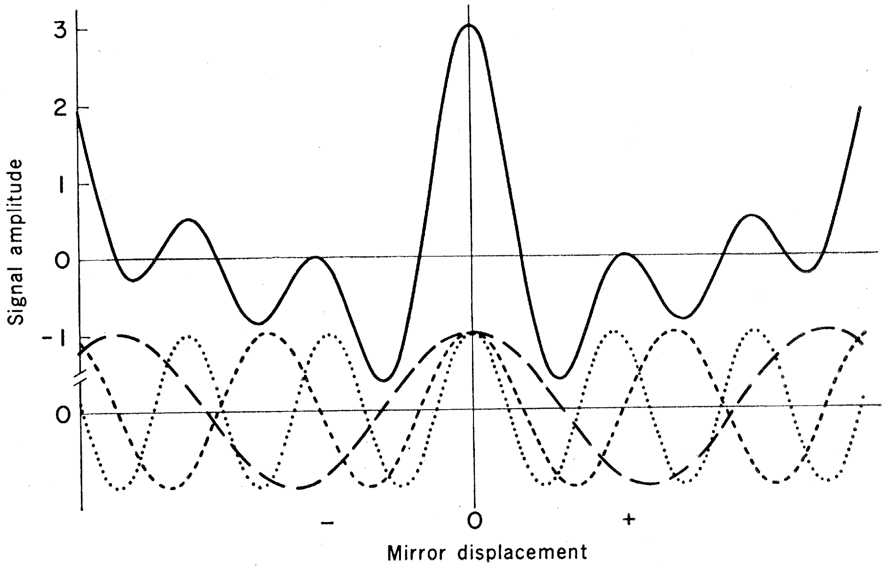

Fig. 2. "Observed" signal from a Michelson interferometer as a function of mirror displacement for an incident wave consisting of three discrete frequencies. This signal is the sum of the three cosine wave signals that would arise from each frequency separately, as indicated. For clarity the individual cosine waves have been displaced downward by two units.

acceptable sampling rate is $2\nu_{max}$ points per second.

Let us see how these ideas apply to an infrared interferogram. The cosine waves with which we are concerned (the component waves in Fig. 2, for example) are functions, not really of time, but of the distance of mirror displacements. Hence the "frequencies" with which we deal are not true frequencies, but wave numbers (in reciprocal centimeters). The commonly studied mid- and far-infrared region of the spectrum extends up to about 4,000 cm^{-1}. If we ensure that no higher frequencies reach the detector by interposing an optical filter with a sharp, high-frequency cutoff, then, according to the sampling theorem, there must be a minimum data acquisition of 8,000 points per centimeter of optical path-length difference (16,000 points per centimeter of mirror displacements since the infrared beam traverses the path to and from the mirror) (*5*).

The question now arises as to how far the mirror must move in obtaining an interferogram. The effect of finite mirror displacement is shown in Fig. 3. We know that a cosine wave of frequency (or wave number) ν_0 and infinite in extent leads, on Fourier transformation, to an infinitely sharp line at ν_0. However, the sharply truncated cosine wave obtained in an actual experiment (Fig. 3C) Fourier transforms to the function shown in Fig. 3D—a line at ν_0 with a finite width and with additional small features in the wings of the line (*6*). From Fourier theory it can be shown that the width of the line at half maximum intensity (in reciprocal centimeters) is given by the reciprocal of the path-length difference (that is, one-half the reciprocal of the mirror displacement). Thus the resolution of the interferometer can, in principle, be made as great as desired by providing sufficient mirror displacement. Optical and mechanical aberrations provide a practical limit—currently about 0.1 cm^{-1} in commercial instruments.

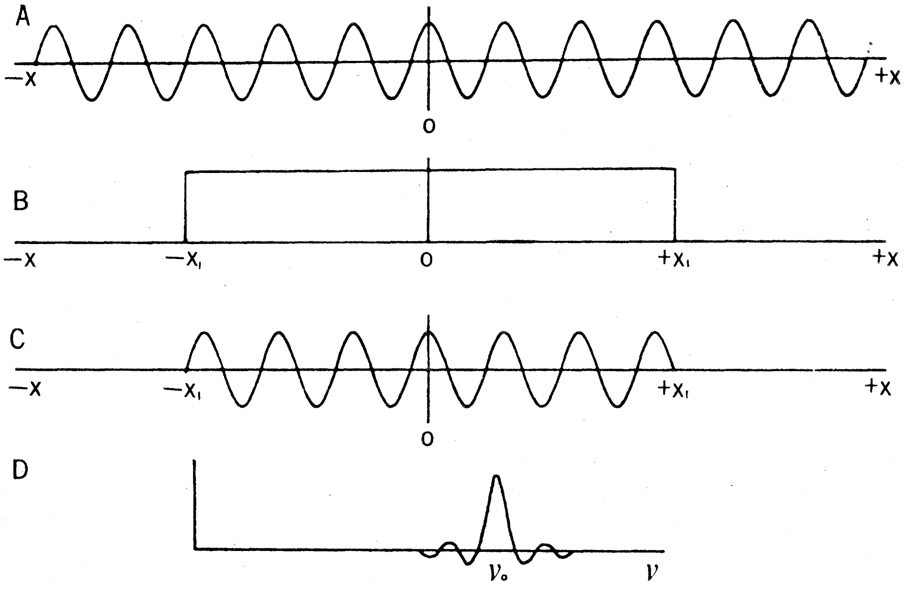

Fig. 3. Effect of the truncation of a cosine wave on the Fourier transform. (A) Cosine wave of infinite extent. (B) Rectangular "window" through which data are taken, limited by the extent of mirror displacement. (C) Actual signal to be transformed. (D) Fourier transform of (C).

We shall not go into the details of instrument design or the availability of commercial FT-IR instruments, but we refer the reader to reviews by Low (*7*) and Horlick (*8*). Many of the computer requirements for FT-IR spectroscopy are similar to those for FT-NMR spectroscopy, which we discuss later.

As an example of the performance of commercial FT-IR spectrometers, we show in Fig. 4 the familiar spectrum of polystyrene, obtained in less than 1 second of instrument time. The efficiency of the interferometric method arises both from the multiplex advantage of obtaining data at all frequencies simultaneously (Fellgett's advantage) and from the larger energy throughput made available by eliminating the narrow slits and small apertures of a monochromator (Jacquinot's advantage) (*9*).

The greatly improved sensitivity now permits study of IR spectra of samples as small as 10 nanograms. The speed of obtaining spectra is being exploited especially in the study of the effluent from gas chromatographs, where the IR spectra of the separate fractions can be obtained in the gas stream.

We now inquire how the advantages of the FT method can be utilized in NMR spectroscopy. A Michelson interferometer is out of the question for a number of reasons; for example, to obtain 1-hertz resolution (3.3×10^{-11} cm^{-1}) the mirror would have to travel over 150,000 kilometers (about one-third of the distance to the moon). But we can achieve the desired goal by using well-known NMR pulse techniques.

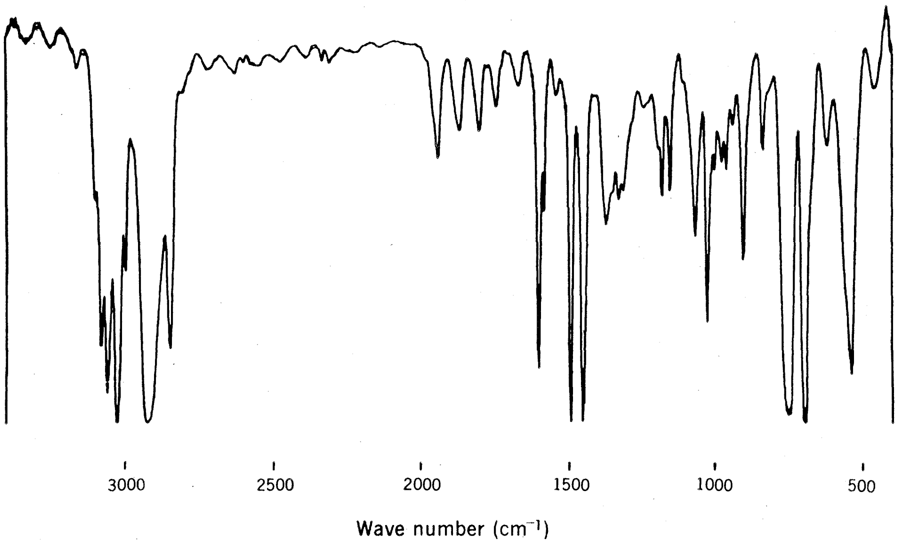

Fig. 4. The speed and reproducibility of a FT-IR spectrometer (Digilab model FTS-14; resolution, 6 cm^{-1}) are demonstrated by the superposition of two spectra of polystyrene, each obtained in less than 1 second of instrument time. [Courtesy of Digilab, Inc., Cambridge, Massachusetts]

Nuclear Magnetic Resonance Pulse Methods

Conventional continuous wave (cw) NMR spectroscopy is similar to other branches of spectroscopy in that a "monochromatic" frequency from a continuously running source is swept through resonance. An alternative method for studying NMR consists of "gating" the transmitter on for a short period in order to apply a short, intense pulse of radio-frequency (rf) energy to the sample. (As we shall see later, this procedure results in a broadband, rather than a monochromatic, source of irradiation.) In order to investigate the effect of the rf pulse, we consider an ensemble of identical nuclei precessing in a magnetic field $\mathbf{H}_0$, as shown in Fig. 5. The nuclear moments are distributed at random in the *x* and *y* directions, and so the resultant macroscopic magnetization **M** is along the *z* axis. Application of a small magnetic field $\mathbf{H}_1$ at right angles to **M** causes **M** to precess about $\mathbf{H}_1$ and to tip toward the *xy* plane. This interaction between $\mathbf{H}_1$ and **M** can occur if $\mathbf{H}_1$ rotates about the *z* axis at the same rate as that at which the nuclei precess, since then $\mathbf{H}_1$ and **M** remain in phase. As long as $\mathbf{H}_1$ is applied, **M** precesses in the *yz* plane at a frequency given by the Larmor relation

$$\omega_R = \gamma H_1 \text{ (in radians per second)}$$

where γ is the magnetogyric ratio of the nucleus. If $\mathbf{H}_1$ is applied for a time t_p, **M** moves through an angle

$$\theta = \gamma H_1 t_p \text{ radians}$$

We thus speak of 90° ($\pi/2$) and 180° (π) pulses, which cause **M** to rotate by those angles.

After application of a 90° pulse, during which $\mathbf{H}_1$ is turned on typically for about 10 microseconds, **M** is along the *y* axis. As **M** precesses, it induces an electrical signal in the coil along the *y* axis. The magnitude of this so-called free-induction signal decreases exponentially with time, as shown in Fig. 6A, since **M** is reduced by natural spin-spin relaxation processes and by the effects of magnetic field inhomogeneity. If the reference frequency used to generate $\mathbf{H}_1$ is not precisely coincident with the resonance frequency, then there is interference between the nuclear signal from the precessing magnetization and the reference signal from the rf oscillator. This leads to the sort of "ringing" pattern shown in Fig. 6B.

Suppose now that the NMR sample has a spectrum consisting of several lines, as in the ^{13}C spectrum of $[^{13}]CH_3I$, shown in Fig. 7A. Then all four of the different NMR frequencies are transmitted simultaneously after the rf pulse. The result is exactly analogous to what happens if, for example, two clarinets that are not in tune sound the "same" note simultaneously—a beat note is obtained whose frequency is equal to the difference between the frequencies played by the two clarinets. For our nuclear sample, there is also a beat frequency, which is equal to *J*, the ^{13}C-H spin-coupling constant, as shown in Fig. 7B. For very simple molecular systems, such as the example given here, the chemical shift and the spin-coupling constant can be obtained quite simply from the time-domain spectrum. Even in this simple case, however, information about the multiplicity of the lines and their relative intensities is not available from simple inspection. For more complicated molecules the time response contains the information in a form too complex to be readily interpreted. As in the IR case, however, Fourier transform methods permit the extraction from the complicated interference pattern of all the information desired on frequencies and amplitudes—that is, the NMR spectrum (*10*). Moreover, as in the IR case, this information can be obtained very rapidly; the free induction decays exponentially with a time constant usually determined by magnetic field homogeneity, typically about 1 second. Although the resolution in the Fourier-transformed spectrum cannot be better than that allowed by field homogeneity, it can be impaired by premature truncation of the data collection, just as in the infrared interferogram. For a resolution of *R* hertz, data must be collected for $1/R$ second.

One aspect of the pulse technique that we have so far not considered is the question of just how nuclei with somewhat different resonance frequencies can be affected by a pulse at one radio frequency. The answer lies in the nature of a short pulse, which on Fourier analysis can easily be shown to contain component frequencies that cover a range approximately the reciprocal of the pulse width. A more quantitative treatment shows that it is really the magnitude of $\mathbf{H}_1$ that is important (*11*) and that, for adequate "coverage" of a frequency range Δ hertz,

$$\gamma H_1/2\pi > \Delta$$

This result can also be expressed in terms of the width of a 90° pulse, t_{90}, as

$$t_{90} < \frac{1}{4\Delta} \text{ second}$$

A sufficiently short pulse, then, is equivalent in some ways to a multitude of separate oscillators that cause the nuclei to "broadcast" their resonance frequencies across the spectrum simultaneously, so that Fellgett's advantage is obtained; specifically this provides a saving in time, or a "time-enhancement factor"

$$\epsilon_t = \Delta/\nu_{1/2}$$

where $\nu_{1/2}$ is the width of a typical line. This reduction in time permits the study of rapid processes, as we illustrate later. Alternatively the sensitivity may be enhanced by the co-addition

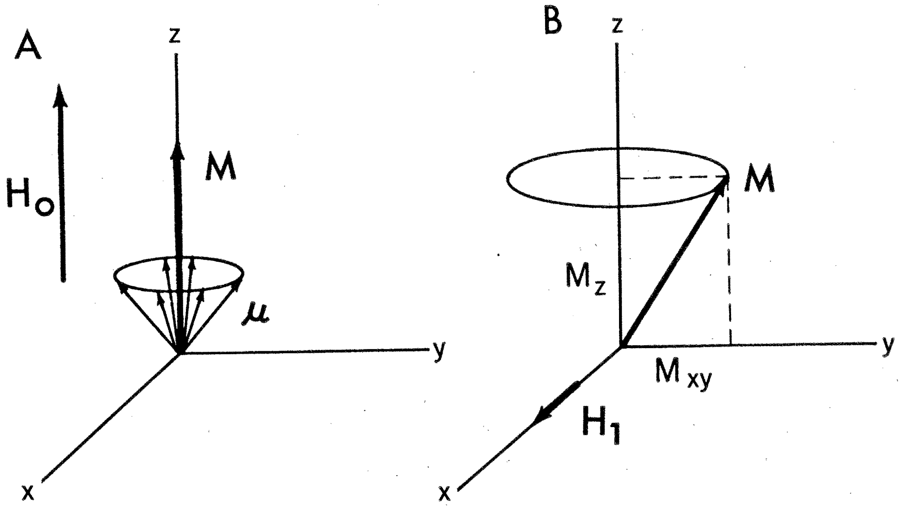

Fig. 5. (A) Precession of nuclear magnetic moments about an applied magnetic field $\mathbf{H}_0$. The resultant macoscopic magnetization **M** is directed along the *z* axis. (B) Tipping of **M** away from the *z* axis by interaction with the rf field $\mathbf{H}_1$. A component of **M** now exists in the *xy* plane and rotates as **M** precesses about $\mathbf{H}_0$.

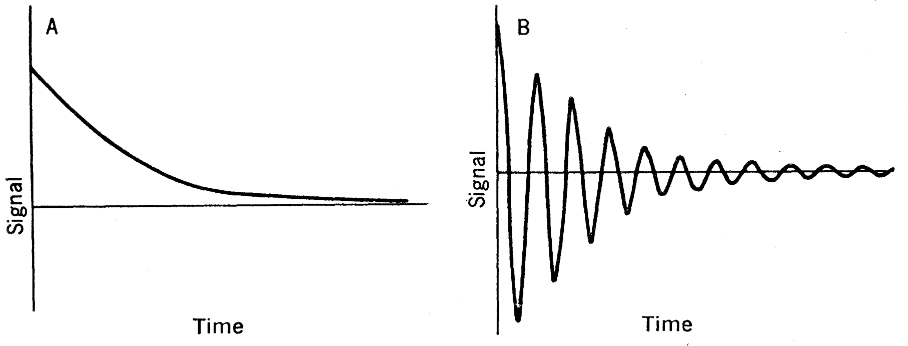

Fig. 6. (A) Exponential decay of the signal after a 90° pulse. (B) Same as (A), except that the rf $\mathbf{H}_1$ and the NMR frequency differ slightly.

of the responses from repeated pulses. For a given length of time a sensitivity enhancement factor,

$$\epsilon_s = \epsilon_t^{1/2} = (\Delta/\nu_{1/2})^{1/2}$$

is obtained from this multiplex advantage.

There is in the NMR pulse method an analog to Jacquinot's advantage in interferometry. In cw NMR studies $\mathbf{H}_1$ must be kept very small, and even at resonance the magnetization $\mathbf{M}$ is not tipped far from the x axis (Fig. 5); hence, M_{xy} is small. With a 90° pulse, however, the entire magnitude of $\mathbf{M}$ is brought into the xy plane, where it induces a large electrical signal in the NMR coil. For repeated pulses, however, this advantage may be reduced by long spin-lattice relaxation times (*11*).

Instrumental and Computer Requirements

We now turn briefly to a consideration of the minimum instrumental and computer requirements for carrying out pulse FT-NMR experiments. Figure 8 shows a block diagram for a simple pulse spectrometer. It consists of a sample probe to contain the sample, an rf transmitter to supply the intense pulse, an oscillator and gate unit to generate the radio frequency and to turn the transmitter on and off, and a pulse programmer which determines when and for how long the transmitter is turned on. The transmitter-gate-probe system has only three basic requirements: (i) it must generate enough power at the probe to satisfy the requirement $\gamma H_1/2\pi > \Delta$; (ii) it must supply a reference signal to the signal-processing system; and (iii) it must return quickly to the equilibrium state (that is, no rf power).

The amplification and detection system must be sensitive over the bandwidth of frequencies to be studied and must recover rapidly (within a few microseconds) from the overload imposed by the strong rf pulse. Further discussion of instrumental aspects of pulse NMR has been given by Farrar and Becker (*11*).

The computer requirements for FT-NMR (and FT-IR) spectroscopy deserve some comment. The Fourier transformation itself is invariably carried out by means of an algorithm developed by Cooley and Tukey, the so-called "fast Fourier transform," which decreases by orders of magnitude the time required for this computation (*12*). Before the transformation is carried out, the computer system (including analog-to-digital converter) must acquire data at the rate specified by the sampling theorem. For nuclei with large chemical shift ranges this rate can be substantial, for example, at least 11,000 data points per second for ^{13}C at 25 megahertz. As we have seen, the time for data acquisition governs the resolution in the final spectrum. In the ^{13}C example, if 0.5-hertz resolution is desired, then a 2-second acquisition time is indicated, and a total of 22,000 data points will be collected. In practice, it is often limitations of computer memory that determine what data acquisition time is to be employed, hence what resolution can be obtained (*13*). The length of a computer word is also an important factor, related to the dynamic range required in the experiment and the number of repetitive scans to be obtained.

In addition to data acquisition and Fourier transformation, the computer is used for several other mathematical operations, namely:

1) "Digital filtering" to improve *S*/*N*.

2) Apodization to correct for line-shape distortions introduced by truncation of the input signal.

3) Correction of frequency-dependent phase errors arising from missetting of the phase-sensitive detector and from distortions caused by the finite width of the pulse and by the electrical filters employed.

4) Display of the selected mode of the spectrum—the usual absorption (v) mode, the dispersion (u) mode, or the power spectrum $(u^2 + v^2)^{1/2}$.

5) Various data-reduction procedures, such as determination and printout of peak positions and intensities.

The computer is thus seen to be an integral part of the FT spectrometer, and most FT-IR and FT-NMR systems include on-line computers to carry out these operations. For economic reasons, however, some installations employ a simple "time-averaging" computer to acquire the data, together with a digital readout of the data in a form suitable for processing by a large off-

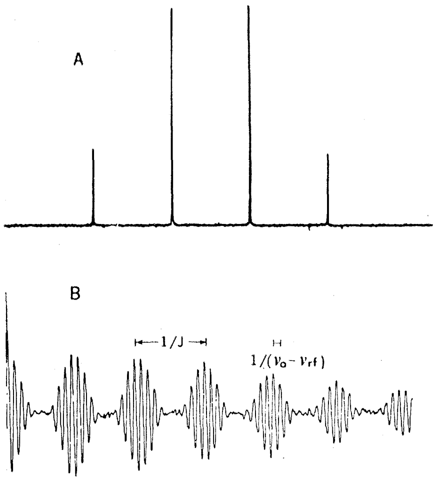

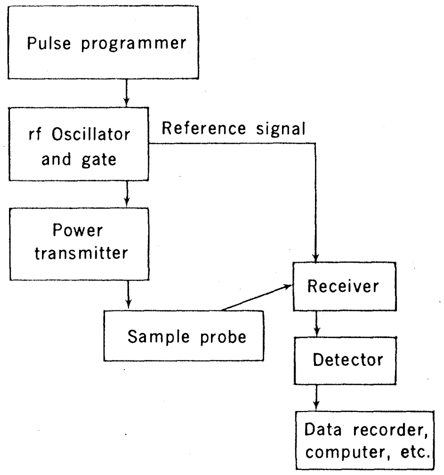

Fig. 7 (left). (A) The ^{13}C spectrum of [^{13}C]CH$_3$I. (B) Free-induction signal observed after application of a 90° pulse to [^{13}C]CH$_3$I. Fig. 8 (right). Block diagram of a simple FT-NMR pulse spectrometer.

line computer. For some applications, it is even possible to dispense with the latter computer and, instead of carrying out a digital Fourier transformation, to use a wave-form analyzer (an analog device) to obtain the power spectrum. In general, the absorption mode spectrum itself is preferred over the power spectrum (*11*), but in some research, including early ^{13}C FT studies (*14*), a wave-form analyzer has been used with success.

Applications of FT-NMR Spectroscopy

The power of the FT method in improving sensitivity is illustrated in Fig. 9, which shows two ^{1}H NMR spectra of 300 micrograms of ergosterol. Figure 9A is the FT spectrum, obtained in 512 seconds, whereas Fig. 9B is the cw spectrum of a 500-second scan. Clearly, with the same amount of instrument time the FT spectrum provides far more information.

Although the use of FT methods to permit ^{1}H NMR studies at submilligram concentrations is of great importance, an even more significant result of the introduction of FT-NMR spectroscopy is that it makes possible the investigation of nuclei with low inherent sensitivity or low natural abundance, or both. During the last 2 years ^{13}C has received special attention. With a natural abundance of 1.1 percent and a sensitivity 1/64 that of ^{1}H, ^{13}C has long been studied only with great difficulty.

In many large organic molecules, especially those of biological interest, ^{13}C FT-NMR spectroscopy can be much more useful than ^{1}H NMR. There are several reasons for this: (i) the ^{13}C chemical shift range is about 200 parts per million (ppm); that for protons is about 10 ppm; (ii) since the carbon atoms are situated in the backbone—or the heart—of organic molecules, they are often more sensitive than protons to the intramolecular environment and the electronic structure of the molecule and are usually much less sensitive to the intermolecular environment; (iii) the C-H dipole-dipole interaction is about 20 times smaller than the H-H dipolar interaction. Thus ^{13}C spectra often have sharper spectral lines and more detail than ^{1}H spectra.

In order to see how these factors can be used to the advantage of chemists and biochemists, let us consider a few examples. Figure 10 shows the ^{13}C FT-NMR spectrum of 4,8-dodecadiene (obtained in about 9 minutes). This molecule is a model compound whose structure has important ramifications for the mechanism of polymerization. The key question concerns the geometry of the protons on the olefinic carbons. Are they both *trans*, both *cis*, or *cis-trans*, as depicted in **I**?

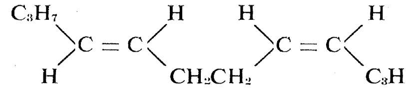
$\mathrm{C_3H_7(H)C{=}C(H)CH_2CH_2(H)C{=}C(H)C_3H_7}$

I

Both the *cis-cis* configuration and the *trans-trans* configuration would give six-line spectra. The actual spectrum, shown in Fig. 10, has 12 lines, one line for each chemically distinct carbon. Clearly the molecule must have the asymmetric *cis-trans* structure of **I**. The ^{1}H spectrum of this molecule gives no useful information.

One of the most exciting potential applications of ^{13}C NMR is to the study of structure and conformation in molecules of biochemical interest. With FT techniques it is possible to study as little as 10-milligram samples of relatively large molecules, such as steroids, with only a few hours needed for data acquisition. More complex biopolymers are also beginning to yield information (*15*). An example of the type of spectra that can be obtained is given in Fig. 11, the FT ^{13}C NMR spectrum of the pentacyclic peptide nisin, which contains 34 amino acid residues (*16*). We shall not discuss the spectral features (these have not yet been interpreted in detail), but we wish to emphasize here the quality of the ^{13}C spectrum obtained in an overnight scan with a solution having a concentration of only 20 m*M*.

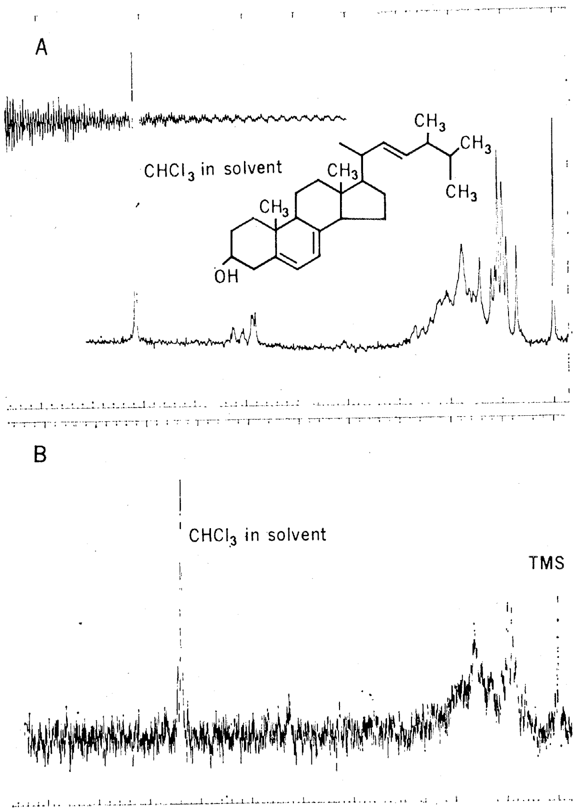

Fig. 9. (A) The ^{1}H FT spectrum of ergosterol (300 micrograms in approximately 0.4 milliliter of $CDCl_3$) at 100 megahertz. This spectrum results from the accumulation of 256 free-induction signals arising from pulses repeated every 2 seconds. (B) The ^{1}H cw spectrum of the same sample; single scan of 500 seconds; *TMS* refers to the peak from tetramethylsilane, which was used as an internal reference. Both spectra were obtained with a JEOL model MH-100 spectrometer. Different frequency scales are used for the two spectra.

Relaxation Measurements

Pulse FT techniques permit facile determination of spin-lattice relaxation times (T_1) for individual NMR spectral lines. The usual procedure consists of the application of a 180° pulse to rotate the equilibrium magnetization to the negative z axis (see Fig. 5), followed after a period τ by a 90° pulse to rotate the magnetization to the y axis to produce a free-induction signal. During the period τ some spin-lattice relaxation occurs, so that the spectrum obtained from Fourier transformation of the free-induction signal is that of the partially relaxed nuclei. Chemically different nuclei of the same species (for example, ^{13}C) may relax at different rates because of differences in their environment or variations in local molecular motions. The relaxation rates of the individual nuclei can then be determined from a series of partially relaxed spectra (*17*), as in Fig. 12. In this case, it is apparent that T_1 for each carbon nucleus depends upon its location in the butyl chain. The α carbons relax much more rapidly than the methyl or distant methylene carbons, which are affected by intrachain, segmental motion. Such relaxation studies add a new dimension to the conventional studies of chemical shifts and coupling constants and should prove especially valuable in spectral assignments of ^{13}C resonances (*18*) and in studies of molecular complex formation.

Stochastic Excitation

Another FT technique for obtaining NMR spectra, stochastic (noise) excitation, deserves brief comment. Instead of using a short pulse to provide a broad-band rf source, pseudorandom noise can be used to modulate the monochromatic rf and thus excite nuclei with a range of resonance frequencies. If this is done, the output noise is no longer random since it contains signals from the nuclear resonances. It has been shown (*19*) that, by taking the cross-correlation between input and output noise and then Fourier-transforming this function, the NMR spectrum is obtained. The saving in time has been shown theoretically to be the same as with the pulse FT method; however, stochastic excitation does not provide the added flexibility of the pulse methods in studies of relaxation times. The instrumentation for stochastic excitation has greater similarity than pulse instrumentation to the instrumentation used for cw NMR spectroscopy, so that modification of existing cw spectrometers may prove easier. Since few papers have been published so far involving the use of this method, the practical advantages and limitations have yet to be determined.

Summary

The recent introduction of Fourier transform methods is revolutionizing IR and NMR spectroscopy. The application of IR interferometry or of NMR pulse methods, followed by Fourier transformation of the resultant interferogram, permits acquisition of spectral data in a time that is orders of

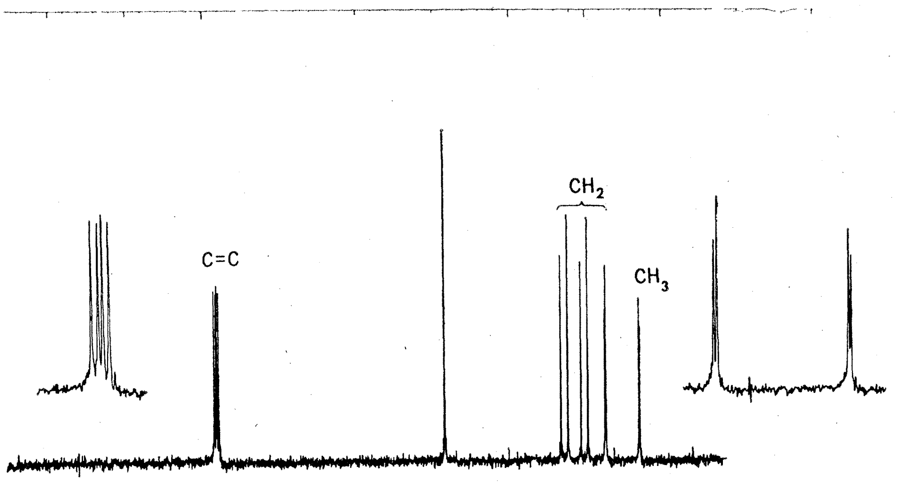

Fig. 10. The ^{13}C FT spectrum of 4,8-dodecadiene at 25 megahertz, resulting from 256 pulses repeated at 2.1-second intervals under conditions of complete ^1H decoupling. The unlabeled peak near the center of the spectrum is from dioxane added to the sample. The insets show abscissa scale expansions for the four lowest frequency peaks and the four highest frequency peaks. A JEOL model PFT-100 spectrometer was used. [Courtesy of Dr. V. Mockel, Firestone Tire and Rubber Company]

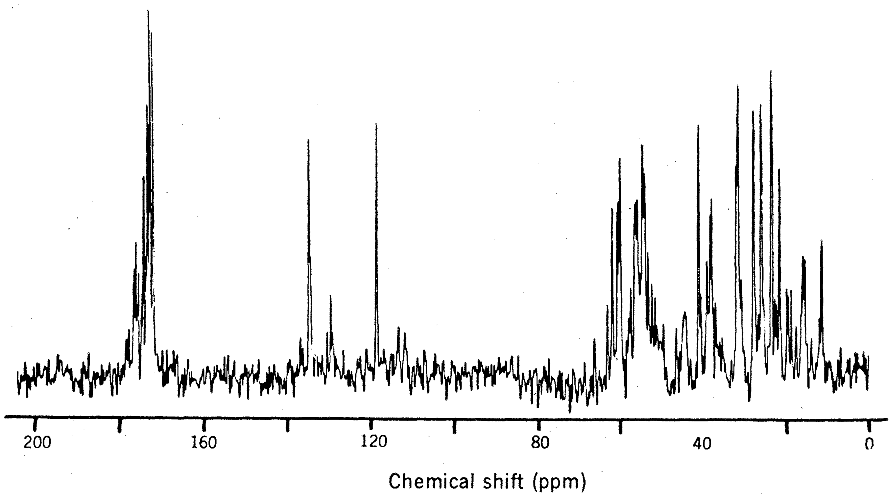

Fig. 11. The 25-megahertz ^{13}C FT spectrum of nisin at a concentration of 0.02*M* in acidified D_2O (*16*). The spectrum results from 60,000 pulses repeated every 0.89 second, over a total data accumulation time of about 15 hours. A JEOL model PFT-100 spectrometer was used.

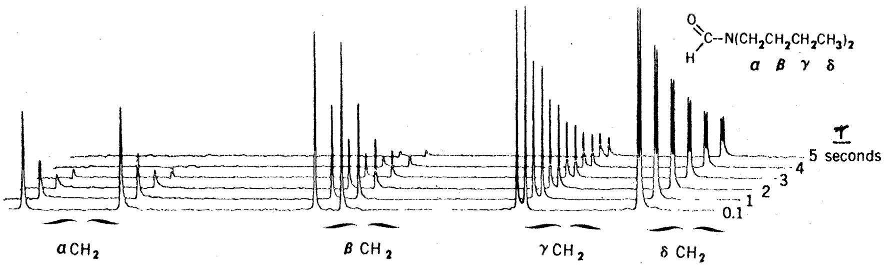

Fig. 12. Partially relaxed 25-megahertz ^{13}C FT spectra (aliphatic carbons only) of di-*n*-butylformamide, obtained by Levy and Nelson (*20*). Each spectrum was produced under complete computer control from a 180°, τ, 90° pulse sequence for the value of τ indicated. The actual plot generated by the computer is the difference between an ordinary equilibrium spectrum (from a single 90° pulse) and the spectrum from the above sequence. The value of T_1 can be obtained from a semilogarithmic plot of signal amplitude versus τ or alternatively can be determined as the value of τ for which the signal has decreased to $1/e$ of its value for $\tau = 0$. A Varian XL-100-FT spectrometer was used. [Courtesy of Dr. G. Levy, General Electric Company]

magnitude less than by conventional spectroscopic methods. This reduction in time permits the study of transient species, or by "time-averaging" procedures *S/N* may be improved without the expenditure of inordinate amounts of time. The FT method finds especially important application in the study of NMR spectra of nuclei of low sensitivity and low abundance, such as ^{13}C.

References and Notes

1. A. A. Michelson, *Phil. Mag.* **31**, 256 (1891); *Studies in Optics* (Univ. of Chicago Press, Chicago, 1927).
2. Fourier transform methods are used in many other areas of science and technology that we shall not touch on here. For example, Fourier analysis has long been a standard technique in the design of electrical circuits and of mechanical systems; holography is a more recent development of FT techniques. Laplace transformation methods recently introduced into electrochemistry [see, for example, A. A. Pilla, *J. Electrochem. Soc.* **117**, 467 (1970); *ibid.* **118**, 1295 (1971)] are also closely related.
3. Prior to the advent of FT methods, conventional time-averaging procedures were used for ^{13}C NMR spectroscopy and in many cases very effectively [see, for example, F. J. Weigart, M. Jautelat, J. D. Roberts, *Proc. Nat. Acad. Sci. U.S.A.* **60**, 1152 (1968)]. For these studies the time was reduced to a manageable level (for example, 12 to 60 hours, rather than 60 days) by sacrificing spectral detail through rapid scanning or by studying only a small portion of the spectrum.
4. See, for example, E. J. Gauss, in *Spectral Analysis*, J. A. Blackburn, Ed. (Dekker, New York, 1970), pp. 28–31.
5. It is apparent that the extension of FT methods to the higher frequency visible or ultraviolet regions of the spectrum presents problems, since very large numbers of data points must be taken per centimeter of mirror displacement, and the precise position of the mirror for each of these points must be determined.
6. The intensity of these "toes" of the line can be reduced by simple mathematical procedures (apodization) but at the expense of a further increase in line width.
7. M. J. D. Low, *Anal. Chem.* **41** (No. 6), 97A (1969); *J. Chem. Educ.* **47**, A163 (1970); *ibid.*, p. A255; *ibid.*, p. A349.
8. G. Horlick, *Appl. Spectrosc.* **22**, 617 (1968).
9. For a good discussion of the history of optical and IR-FT spectroscopy, see E. V. Loewenstein, *Appl. Opt.* **5**, 845 (1966).
10. R. R. Ernst and W. A. Anderson, *Rev. Sci. Instrum.* **37**, 93 (1966).
11. See, for example, T. C. Farrar and E. D. Becker, *Pulse and Fourier Transform NMR* (Academic Press, New York, 1971).
12. For a discussion of the rationale and speed of this calculation, see, for example, W. T. Cochran *et al.*, *Proc. Inst. Electr. Electron. Eng.* **55**, 1664 (1967).
13. If the spectrum for a particular sample is known to cover a small frequency range, or if the range of frequencies can be limited by a sharp-cutoff, low-pass filter, then data sampling rates can, of course, be reduced. Within the limitation imposed by computer memory, better resolution can thus be obtained.
14. D. Jones and H. Sternlicht, paper presented at the 11th Experimental NMR Conference, Pittsburgh, Pennsylvania, 21 April 1970.
15. See, for example, A. Allerhand, D. Doddrell, V. Glushko, D. W. Cochran, E. Wenkert, P. J. Lawson, F. R. N. Gurd, *J. Amer. Chem. Soc.* **93**, 544 (1971).
16. E. Gross and J. L. Morell, *ibid.* **92**, 2919 (1970).

→ R. L. Vold, J. S. Waugh, M. P. Klein, D. E. Phelps, *J. Chem. Phys.* **48**, 3831 (1968).

18. A. Allerhand and D. Doddrell, *J. Amer. Chem. Soc.* **93**, 2777 (1971).
19. R. R. Ernst, *J. Magn. Resonance* **3**, 10 (1970); R. Kaiser, *ibid.*, p. 28.
20. G. C. Levy and G. L. Nelson, *J. Amer. Chem. Soc.*, in press.
21. We thank Dr. E. Gross, National Institutes of Health, for supplying the sample of nisin used to obtain the spectrum of Fig. 11. We thank Dr. V. Mockel, Firestone Tire and Rubber Company, for permission to use the spectrum shown in Fig. 10 and Dr. G. Levy, General Electric Company, for permission to use the spectrum shown in Fig. 12.

The Ortega Hypothesis

Citation analysis suggests that only a few scientists contribute to scientific progress.

Jonathan R. Cole and Stephen Cole

Most scientists are aware that science is a highly stratified institution. Power and resources are concentrated in the hands of a relatively small minority. For the past several years we have been studying the social stratification system of science (*1–3*). Most of our research has concentrated on the social processes through which individual scientists are evaluated, to discover why some scientists rise quickly to positions of eminence and others remain relatively obscure. Two conflicting theories explain social mobility in science. According to one theory the stratification system of science operates on strictly universalistic criteria: the scientists who publish the most significant work receive the ample recognition they deserve; those not publishing significant work are ignored. According to the other theory, a small elite at a handful of universities and government-supported laboratories control the social institutions of science in such a way as to perpetuate their own ideas and assure the social mobility of their intellectual children. The results of our research have for the most part supported the former theory. We have found that quality of published research explains more variance than any other variable on several types of recognition.

Contributions from Scientific Strata to Progress in Science

Whereas most of our previous research has dealt with the processes through which individuals find their level in the stratification system, in this article we analyze another problem. We present data evaluating the comparative contributions of the various scientific strata to scientific progress, indicating whether progress is built on the labor of all "social classes" or is primarily dependent on the work of an "elite." In the past, historians and philosophers of science have attributed much of the growth of science to the work of the average scientist, who, it is suggested, has paved the way with his "small" discoveries for the men of genius—the great discoverers. This hypothesis is asserted in many sources, but perhaps no more clearly than in the words of Jose Ortega y Gasset (*4*):

> For it is necessary to insist upon this extraordinary but undeniable fact: experimental science has progressed thanks in great part to the work of men astoundingly mediocre, and even less than mediocre. That is to say, modern science, the root and symbol of our actual civilization, finds a place for the intellectually commonplace man and allows him to work therein with success. In this way the majority of scientists help the general advance of science while shut up in the narrow cell of their laboratory, like the bee in the cell of its hive, or the turnspit of its wheel.

Dr. Jonathan R. Cole is assistant professor of sociology at Columbia University, New York 10027. Dr. Stephen Cole is associate professor of sociology at the State University of New York (SUNY) at Stony Brook, New York 11790. This article is based on a paper read at the AAAS meeting in Chicago, Illinois, on 28 December 1970.